

Dark matter decay and the abundance of ultracompact minihalos

YU-PENG. YANG^{1,2,3} (a), GUI-LIN. YANG^{1,3} (b) and HONG-SHI. ZONG^{1,3,4} (c)

¹ *Department of Physics, Nanjing University - Nanjing, 210093, China*

² *School of Astronomy and Space Science, Nanjing University - Nanjing, 210093, China*

³ *Joint Center for Particle, Nuclear Physics and Cosmology - Nanjing, 210093, China*

⁴ *State Key Laboratory of Theoretical Physics, Institute of Theoretical Physics, CAS, Beijing 100190, China*

PACS 98.80.-k – Cosmology

PACS 95.36.+x – Dark matter, dark matter decay and dark matter halos

PACS 98.80.Cq – Early Universe, dark matter halos are formed in the early universe

Abstract – Ultracompact minihalos would be formed if there are larger density perturbations ($0.0003 < \delta\rho/\rho < 0.3$) in the earlier epoch. The density profile of them is steeper than the standard dark matter halos. If the dark matter can annihilate or decay into the standard particles, e.g., photons, these objects would be the potential astrophysical sources. In order to be consistent with the observations, such as *Fermi*, the abundance of ultracompact minihalos must be constrained. On the other hand, the formation of these objects has very tight relation with the primordial curvature perturbations on smaller scale, so the fraction of ultracompact minihalos is very important for modern cosmology. In previous works, the studies are focused on the dark matter annihilation for these objects. But if the dark matter is not annihilated, the dark matter decay is another important possible case. On the other hand, the abundance of ultracompact minihalos is related to many other parameters, such as the mass of dark matter, the decay channels and the density profile of dark matter halo. One of the important aspects of this work is that we investigate the γ -ray signals from nearby ultracompact minihalos due to dark matter decay and another important aspect is to study in detail how the different decay channels and density profiles affect the constraints on the abundance of ultracompact minihalos.

Introduction. – The structure formation is one of the important fields of modern cosmology. It is well known that the present structures of our observational cosmos come from the earlier density perturbations which is produced during the inflation. The amplitude of these density perturbations are $\delta\rho/\rho \sim 10^{-5}$. If the density perturbations at earlier epoch are larger than 0.3, the primordial black holes (PBHs) would be formed [1]. Recently, Ricciotti and Gould proposed that if the density perturbations are larger than 10^{-3} but smaller than 0.3, one new kind of dark matter structure called ultracompact minihalos (UCMHs) would be formed [2]. The formation time of these objects is earlier and the density is larger than the standard dark matter halos. If the dark matter particles consist of weakly interacting massive parti-

cles (WIMPs), it is expected that UCMHs would have notable effect on the cosmological evolution due to the dark matter annihilation or decay. In Refs. [3–5], the authors studied the impact of UCMHs on the cosmological ionization and obtained the constraints on the abundance of them. If high energy photons are produced by the dark matter annihilation, the UCMHs will become one kind of astrophysical sources and they can contribute to the γ -ray background [6–12]. The authors of Refs. [6–8] investigated these effects and obtained the constraints on the fraction of UCMHs. They found that the strongest constraint is $f_{\text{UCMHs}} \sim 4 \times 10^{-7}$ for the mass of UCMHs $M_{\text{UCMHs}} \sim 7 \times 10^3 M_{\odot}$. In Ref. [9], the authors investigated the contributions of UCMHs to the extragalactic gamma-ray background and found that the constraints increase with the dark matter mass: $f_{\text{UCMHs}} \sim 10^{-5}$ and $\sim 10^{-3}$ for the dark matter mass $M_{\chi} \sim 10\text{GeV}$ and $\sim 1\text{TeV}$, respectively. These constraints are stronger than the results obtained from the CMB data by about one or-

(a) E-mail: yyp@chenwang.nju.edu.cn

(b) E-mail: yanggl@chenwang.nju.edu.cn

(c) E-mail: zonghs@chenwang.nju.edu.cn

¹Actually, this value depends on the redshift and the scale of density perturbations. For more details one can see Ref. [8].

der of magnitude (see the Fig. (4) in Ref. [9]).² If the dark matters are not annihilated, due to the steep density profile of UCMHs, they would be detected by microlensing observations [14]. The formation of UCMHs has very closer relation with many aspects, such as the primordial density perturbations on the smaller scales ($k = 5 \sim 10^8 \text{ Mpc}^{-1}$) which cannot be constrained by the cosmic microwave background (CMB), LSS and Lyman- α (see the Fig. (6) of Ref. [8]). Moreover, the UCMHs can also be used to constraints the non-gaussianity [13], so the fraction of UCMHs is very important for modern cosmology.

As the necessary component of cosmology, dark matter has been confirmed by many observations. But the essence of them is still unknown and there are many models at present. One of the important models is that they are composed of WIMPs, such as neutralino, which comes from the supersymmetric extension of the standard model [15–17]. According to this theory, they are stable and can annihilate into the standard particles. Except for these "annihilation models", there are also other models and one important of them is "decay models", e.g. decaying gravitinos in R-parity violating SUSY models [18, 19]. These particles are unstable and can also decay into the standard particles. The lifetime of them is usually longer or comparable than the cosmic age. All of the previous works mainly focused on the impact of UCMHs due to the dark matter annihilation. But, as was mentioned above, if the dark matters are not annihilated, the decay would be another important possible case, and it will be considered in this work firstly for UCMHs. We use the WMAP-7 years data to obtain the constraints on the decay rate $\Gamma(s^{-1})$ (or the lifetime $\tau(s)$) and then use these results to perform the following calculations.

Another important factor which affects the final constraints on the abundance of UCMHs is the density profile of Milky Way's dark matter halo. The density profile of dark matter halo has been "determined" by simulations and observations. One of the popular models is the NFW profile which is obtained through the simulations [20]. But it diverges in the center as $r \rightarrow 0$, and this can be avoided by other models, such as isothermal [21] and Einasto [22]. On the other hand, there are also many observations to constrain the density profile [23–25]. For the abundance of UCMHs, because the final constraints are related to the density profile of dark matter halo, in this work we will investigate how the different density profiles affect the fraction of UCMHs.

This paper is organized as follows. In Sec. II we show the integrated γ -ray flux from UCMHs due to dark matter decay. In Sec. III we discuss how the related parameters affect the constraints on UCMHs fraction and the conclusion is given in Sec. IV.

The γ -ray signals from UCMHs due to dark matter decay. – After UCMHs are seeded during the radi-

ation dominated epoch, the dark matter particles will be accreted by the radial infall. The mass of UCMHs changed slowly until the matter is dominated. It can be written in the form [2, 6]

$$M_{\text{UCMHs}}(z) = M_i \left(\frac{1 + z_{\text{eq}}}{1 + z} \right), \quad (1)$$

where M_i is the mass within the perturbation scale at the time of matter-radiation equality.

The density profile can be obtained through the simulation [2, 26, 27]

$$\rho(r, z) = \frac{3f_\chi M_{\text{UCMHs}}(z)}{16\pi R(z)^{\frac{3}{4}} r^{\frac{9}{4}}}, \quad (2)$$

where $R(z) = 0.019 \left(\frac{1000}{z+1} \right) \left(\frac{M(z)}{M_\odot} \right)^{\frac{1}{3}} \text{ pc}$ and $f_\chi = \frac{\Omega_{DM}}{\Omega_b + \Omega_{DM}} = 0.83$ [28] is the dark matter fraction. Due to the structure formation effect, the mass of UCMHs will stop increasing at recent time and in this work we assumed the corresponding redshift is $z = 10$ [6, 8]. The radius of UCMHs is $R(z = 10) \sim 0.01 M_i^{\frac{1}{3}}$ and $R \sim 1 \text{ kpc}$ for $M_i = 10^6 M_\odot$. So in the following discussions we will also treat the UCMHs as point sources [2, 6, 8]. The density profile of UCMHs is obtained by assuming the perfect radial infall. But after the formation of UCMHs, it is not always the true cases and the angular momentum will be important. It means that this effect will make the density at the center smaller and a core would be formed instead of $\rho \rightarrow \infty$ for $r \rightarrow 0$. We accept the analysis process in Ref. [8] and set the minimum radius $r_{\text{min}} \sim 10^{-7} (M_{\text{UCMHs}(z=0)} / M_\odot)^{-0.06} R_{\text{UCMHs}(z=0)}$. For the smaller radius, we assume that the density is a constant $\rho_{r < r_{\text{min}}} = \rho(r_{\text{min}})$. The integrated flux of γ -ray signals from nearby UCMHs can be written as

$$\Phi = \frac{1}{4\pi d^2} \frac{\Gamma}{m_\chi} \sum^i \int_{E_{\text{th}}}^{m_\chi} B_{f_i} \frac{dN_i}{dE} dE \int \rho(r) d^3r \quad (3)$$

where the summation is for all decay channels, d is the distance from the earth. $\frac{dN}{dE}$ is the energy spectrum of dark matter decay, which can be obtained by the public code: DarkSUSY³. B_{f_i} is the branching ratio of each decay channel. In this work, we consider each decay channel separately and set $B_f = 1$. The E_{th} is the threshold value of the detector. Here we consider the *Fermi* observation and choose the threshold value $E_{\text{th}} = 100 \text{ MeV}$. In Fig. 1, the integrated γ -ray signals above 0.1 GeV from UCMH are shown. Two decay channels are plotted: $b\bar{b}$ and $\tau^+\tau^-$. For the decay rate, we have chosen $\Gamma = 10^{-26} \text{ s}^{-1}$ and the distance of UCMH is $d = 10 \text{ kpc}$. In order to compare with the observations, the point source sensitivity of *Fermi* are also shown⁴ ($\Phi_{(E > 100 \text{ MeV})} = 4.0 \times 10^{-9} \text{ cm}^2 \text{ s}^{-1}$ for one year observation times, 5σ confidence level). From

²For both cases, the constraints on the UCMHs abundance are independent of the mass of UCMHs.

³<http://www.physto.se/edsjo/darksusy/>

⁴ <http://fermi.gsfc.nasa.gov/science/instruments/table1-1.html>

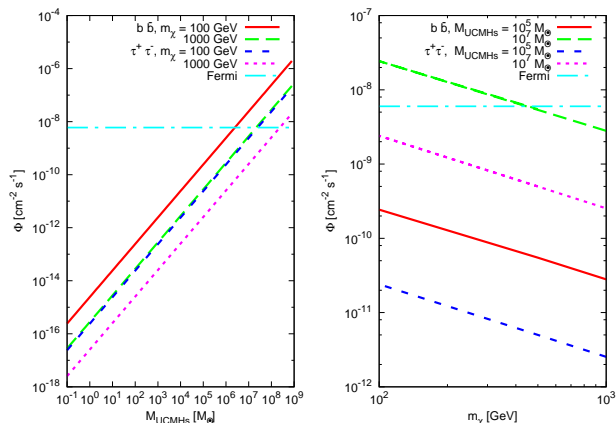


Fig. 1: The integrated γ -ray signals above 0.1 GeV from nearby UCMH ($d = 10$ kpc) due to dark matter decay. Two decay channels are shown: $b\bar{b}$ and $\tau^+\tau^-$ and the decay rate is $\Gamma = 10^{-26} \text{ s}^{-1}$. The point source sensitivity of *Fermi* are also shown.

the figure one can see that the integrated flux is proportional to the mass of UCMHs ($\Phi \propto M_{\text{UCMHs}}$) and inversely proportional to the dark matter mass ($\Phi \propto 1/m_\chi$). Actually, these characters can be seen apparently from Eq. (3). Therefore, for the fixed distance, the final flux would exceed the point source sensitivity of *Fermi* for the larger UCMHs mass or smaller dark matter mass. On the other hand, it also can be seen that the final flux depends on the decay channels while the difference are not very large [8]. Moreover, one should realize that the integrated flux is also related to the dark matter decay rate which now have been constrained by many observations [29–38].

Constraints on the Fraction of UCMHs. – If one single UCMH exists in the Milky Way dark matter halo, the upper limits on the fraction of UCMHs for the non-detection results (e.g. *Fermi*) can be written as [7], $f_{\text{UCMHs}} = \frac{M_{\text{UCMHs}}(z=0)}{M_{\text{DM}}(r < d_{\text{obs}})}$, where d_{obs} is the distance that the γ -ray signals from UCMHs can be observed by the detector and $M_{\text{DM}}(r < d_{\text{obs}})$ is the mass of Milky Way within this radius. On the other hand, if UCMHs indeed exist within the distance d_{obs} , but they are not observed due to the limitation of the detector, the upper limits on the fraction of UCMHs will become [8]

$$f_{\text{UCMHs}} = \frac{f_\chi M_{\text{UCMHs}}(z=0)}{M_{\text{MW}}} \frac{\log(1 - y/x)}{\log(1 - M_{d < d_{\text{obs}}}/M_{\text{MW}})} \quad (4)$$

where y and x are the confidence level corresponding to the f_{UCMHs} and the detector, respectively. M_{MW} is the dark matter halo mass of Milky Way. More general and slightly improved form is presented in Ref. [13] (eq. A2). We find that the corresponding changes of the results for our work can be neglected safely. We also consider the limits from the galactic diffuse emission which is very important for the smaller UCMHs. For the very large distance of

UCMHs, the constraints from the extragalactic sources are also considered (for more details, one can see Eqs.(28) and (29) in Ref. [8]). Following Ref. [33], we use three kinds of density profile for the Milky Way, NFW, Isothermal (Iso), Einasto (Ein) and use the value of parameters in that reference. We also assume that the abundance of UCMHs is the same everywhere [6, 8].

From the discussions in Section 2, it can also be seen that several parameters can affect the final integrated γ -ray flux. So, the final constraints on the abundance of UCMHs will also be affected by these parameters. In this section, we will discuss in detail how these parameters affect the final constraints. One of the important parameters is the dark matter decay rate (Γ). It has no theoretically defined value but has to be constrained by observations. There are many ways to give the constraints on this parameters including using the extragalactic γ -ray or CMB. In this work, we use the WMAP-7 years data to obtain the constraints on the decay rate. For the detailed discussions on the effect of dark matter decay on the CMB one can see Ref. [39]. Here we only give a general description. The dark matter can decay into the standard particles such as photons (γ), electrons (e^-) and positrons (e^+) and so on. These particles will have interaction with the content of cosmos, such as the interaction between the photons and the hydrogen atoms which are formed after the recombination ($z \sim 1100$). One of the effects is to delay the recombination. Moreover, the dark matter decay would be one kind of sources of reionization. Therefore, the evolution of ionization fraction including the dark matter decay can be written as [39]

$$\frac{dx_e}{dz} = \frac{1}{(1+z)H(z)} [R_s(z) - I_s(z) - I_{\text{DM}}(z)] \quad (5)$$

where R_s and I_s are the standard recombination rate and ionization rate. I_{DM} is the ionization rate from the dark matter decay and it is related to the decay rate $I_{\text{DM}} \propto \zeta\Gamma$, where ζ stands for the fraction of the energy which has been injected into the baryonic gas by the dark matter decay. The effect of the dark matter decay on the evolution of ionization fraction will influence the power spectrum of CMB and we can use the WMAP data to obtain the constraints on the decay rate. We modified the public code CAMB⁵ to include the effect of dark matter decay and the code COSMOMC⁶ to obtain the constraints on the parameters. We use the seven years WMAP data [41], and the data from ACBAR [42], Boomerang [43], CBI [44] and VSA [45] experiments and 7 cosmological parameters, $\{\Omega_b h^2, \Omega_d h^2, \theta, \tau, n_s, A_s, \zeta\Gamma\}$, where $\Omega_b h^2$ and $\Omega_d h^2$ are the density of baryon and dark matter, θ is the ratio of the sound horizon at recombination to its angular diameter distance multiplied by 100, τ is the optical depth, n_s is the spectral index and A_s is the amplitude of the primordial

⁵<http://camb.info/>

⁶<http://cosmologist.info/cosmomc/>

density perturbation power spectrum. For the constraints on the dark matter decay rate, following the methods in Refs. [39,40], we have used a flat prior for $\zeta\Gamma(\times 10^{-26}s^{-1}) : [0, 100.]$ and it is enough for our purpose. The final results are listed in Tab. 1. From these results, we can obtain the constraints on the decay rate for the WMAP-7 years: $\zeta\Gamma < 0.77 \times 10^{-25}s^{-1}(2\sigma)$. Generally speaking, ζ depends on the redshift and different decay channels. In the following work, we set $\zeta = 1$ and this is enough for our consideration. The dark matter decay rate can also be constrained by the gamma-ray or the X-ray observations. Generally speaking, these results depend on the decay channels and the density profile of dark matter halos. For some decay channels, the limits on the decay rate are stronger than our results. For example, for the gamma-ray observations of the Fornax by the *Fermi*, the limit on the dark matter lifetime for the $b\bar{b}$ channel is $\tau \sim 4 \times 10^{26}s$ for the dark matter mass $m_\chi \sim 300$ GeV [37]. All these results can be applied easily to our work.

In this work, we consider two typical decay channels: $b\bar{b}$ and $\tau^+\tau^-$. In order to obtain the final constraints, we first obtain the distance (d_{obs} in Eq. (4)) for the fixed UCMHs mass where the integrated gamma-ray flux does not exceed the point source sensitivity of *Fermi*, and then we can use Eq. (4) to obtain the final results. The final constraints on the fraction of UCMHs for 95% confidence level for different dark matter mass, decay channels, decay rate and density profiles are shown in Fig. 2.

From Fig. 2, it can be seen that the strongest constraints comes from the $b\bar{b}$ channel and the dark matter mass $m_\chi = 100$ GeV. The corresponding fraction is $f_{UCMHs} \sim 5 \times 10^{-5}$ with the mass of UCMHs $M_{UCMHs} \sim 10^6 M_\odot$. For a fixed mass of dark matter and UCMHs, the constraints for the lepton decay channels are weaker. This is due to the smaller integrated photon number for these decay channels. For a fixed density profile of Milky Way's dark matter halo and dark matter mass, the limits for the fraction are weaker for the smaller decay rate (longer lifetime). It can also be seen that the constraints obtained in this work are weaker than those of other works which considered the case of dark matter annihilation [7,8]. The main reason is that the strength of dark matter decay is proportional to the density rather than the density squared. One should note that even though the final results are weaker than the cases of annihilation, however, if the dark matter are not annihilated, then the decay could be another very important case. So, the constraints obtained by us are also very significant for the dark matter decay models.

The constraints on the fraction of UCMHs can be translated into the limits on the primordial curvature perturbations on smaller scales. The process of calculation is given in Ref. [8]. In this work, we follow their methods and give the conservative limits on the primordial curvatures perturbations which are shown in Fig. 3. ⁷ For this

plot, we set the dark matter mass $m_\chi = 1$ TeV and choose the $b\bar{b}$ decay channel and NFW dark matter halo model for the Milky Way. For the decay rate, we have used two values, $\Gamma = 7.7 \times 10^{-26}s^{-1}$ which has been obtained by us using the CMB data, and $\Gamma = 1.0 \times 10^{-27}s^{-1}$ which corresponds to the allowed value obtained from other observations (e.g. gamma-ray observations [38]). Moreover, the latter value is also within the allowed regions obtained by us. From this figure it can be seen that the strongest limit is $\mathcal{P}_{\mathcal{R}}(k) \sim 1.7 \times 10^{-6}$ for $k \sim 10^{2.2} \text{Mpc}^{-1}$. For the smaller decay rate (longer lifetime), the limits are weaker.

Conclusions. – If the dark matter are not annihilated, the decay model would be another important case. So, it is expected that the UCMHs would contribute to the γ -ray flux due to the dark matter decay within them. On the other hand, the abundance of UCMHs is very important for modern cosmology. For example, it can be used to constrain the primordial curvature perturbations on small scales. In this work, we first investigated the integrated γ -ray flux from nearby UCMHs due to the dark matter decay. In the case of larger mass of UCMHs or smaller dark matter mass, e.g. $m_\chi = 200$ GeV, $M_{UCMHs} = 10^7 M_\odot$ and $b\bar{b}$ decay channel, the integrated γ -ray flux from the distance $d = 10$ kpc would achieve the point source sensitivity of *Fermi*. Another important aspect is that we have studied the influence of different decay channels and density profiles of dark matter halo on the constraints of UCMHs abundance. One of the important parameters is the dark matter decay rate (Γ). Since the cosmological evolution, e.g. reionization, can be affected by the dark matter decay, this parameter can be constrained by the CMB observations. In this work, we have used the WMAP-7 years data to obtain the constraints and used these results to perform the following calculations. We considered two decay channels: $b\bar{b}$, $\tau^+\tau^-$ and assumed each of the branching ratio $B_f = 1$. For the density profile of dark matter halo, we used NFW, Isothermal and Einasto models to obtain the final constraints. We found that the strongest constraints on the fraction of UCMHs comes from the smaller dark matter mass and the $b\bar{b}$ channel where $f_{UCMHs} \sim 5 \times 10^{-5}$ for $M_{UCMHs} \sim 10^6 M_\odot$. For all these three kinds of density profile, the strongest constraints are similar. The constraints on the fraction of UCMHs can be translated into the limits on the primordial curvature perturbations on smaller scales. We found that the strongest conservative limit is $\mathcal{P}_{\mathcal{R}}(k) \sim 1.7 \times 10^{-6}$ for $k \sim 10^{2.2} \text{Mpc}^{-1}$ for the specific parameters of dark matter particles and the dark matter halo model. Although these results are weaker than the cases of dark matter annihilation, they are still very useful if the dark matter particles are not annihilated.

Yang Yu-Peng thank Sun Weimin for improving the manuscript. We thank the referees for their very useful

⁷Detailed discussions for these constraints are prepared for an-

other work.

Table 1: Posterior constraint on the cosmological parameters including dark matter decay from WMAP-7 years observation.

Parameters	$100\Omega_b h^2$	$\Omega_c h^2$	θ_S	τ	$\Gamma(\times 10^{-24} s^{-1})$	n_s	$\log[10^{10} A_s]$
mean	2.231	0.119	1.040	0.075	0.035	0.958	3.113
2σ lower	2.143	0.113	1.036	0.042	0.000	0.937	3.050
2σ upper	2.321	0.125	1.104	0.105	0.077	0.980	3.178

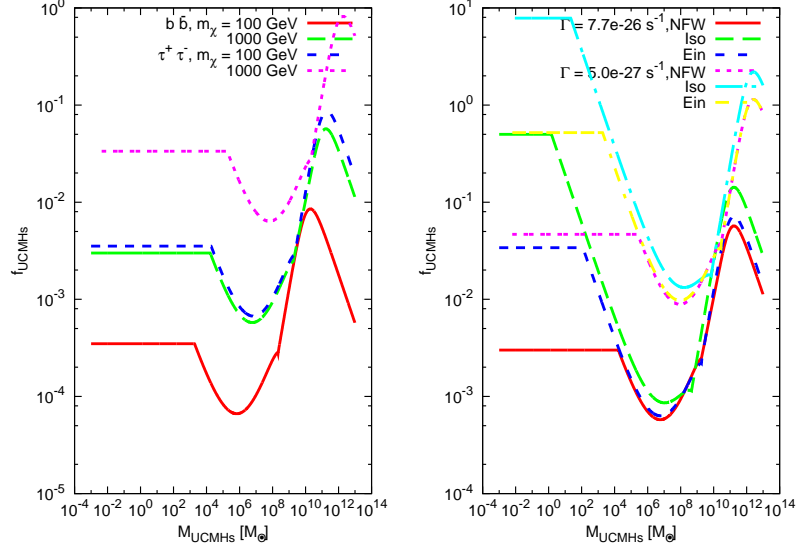


Fig. 2: Upper limits on the fraction of UCMHs for different dark matter mass, decay channels, density profile and decay rate. Left: two dark matter mass $m_\chi = 100$ GeV, 1 TeV and decay channels $b\bar{b}$, $\tau^+\tau^-$ for NFW density profile for our Milky Way dark matter halo are shown. For this plot, the dark matter decay rate is $\Gamma = 7.7 \times 10^{-26} s^{-1}$. Right: different dark matter decay rate $\Gamma = 7.7 \times 10^{-26} s^{-1}$, $5.0 \times 10^{-27} s^{-1}$ and density profile for our Milky Way dark matter halos NFW, Iso, Ein are shown. In this figure, we have fixed the decay channel $b\bar{b}$ and dark matter mass $m_\chi = 1$ TeV.

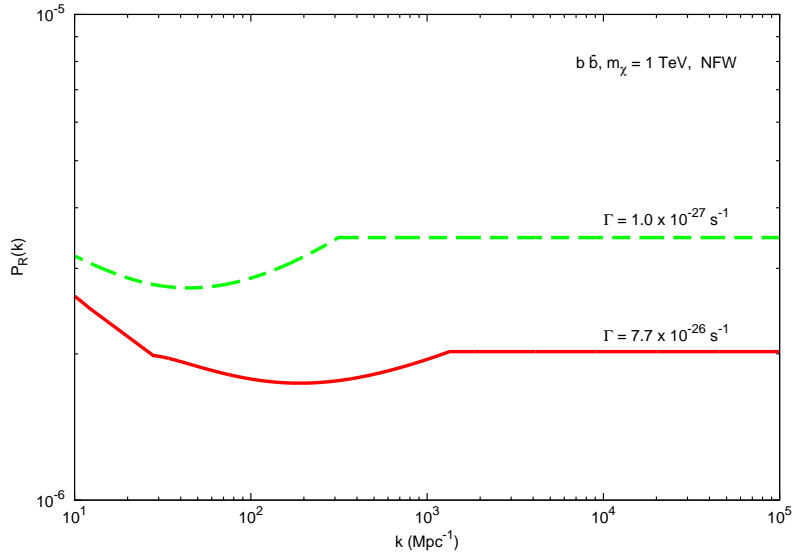


Fig. 3: Conservative limit on the primordial curvature perturbations obtained for the dark matter mass $m_\chi = 1$ TeV and $b\bar{b}$ channel, and NFW density profile for our Milky Way dark matter halo. Here, we have set $\delta_{\min} = 0.006$ which corresponds to the largest value obtained in [8] for the formation of UCMHs at all scales.

suggestions. Our MCMC chains computation was performed on the Shenteng 7000 system of the Supercomputing Center of the Chinese Academy of Sciences. This work is supported in part by the National Natural Science Foundation of China (under Grant Nos 10935001 and 11075075).

REFERENCES

- [1] GREEN A. G. and LIDDLE A. R., *Phys. Rev. D*, **56** (1997) 6166.
- [2] RICOTTI M. and GOULD A., *Astrophys. J.*, **707** (2009) 979.
- [3] YANG Y., HUANG X., CHEN X., and ZONG H., *Phys. Rev. D*, **84** (2011) 043506.
- [4] YANG Y., CHEN X., LU T. and ZONG H., *Eur. J. Phys. Plus*, **126** (2011) 123.
- [5] ZHANG D., *MNRAS*, **418** (2011) 1850.
- [6] SCOTT P. and SIVERTSSON S., *Phys. Rev. Lett.*, **103** (2009) 211301.
- [7] JOSAN A. S. and GREEN A. M., *Phys. Rev. D*, **82** (2010) 083527.
- [8] BRINGMANN T., SCOTT P. and AKRAMI Y., *Phys. Rev. D*, **85** (2012) 125027.
- [9] YANG Y., FENG L., HUANG X., CHEN X., LU T. and ZONG H., *JCAP*, **12** (2011) 020.
- [10] BEREZINSKY V., DOKUCHAEV V., EROSHENKO Y., KACHELRIESS M., and SOLBERG M. A., *Phys. Rev. D*, **81** (2010) 103529.
- [11] BEREZINSKY V., DOKUCHAEV V., EROSHENKO Y., KACHELRIESS M., and SOLBERG M. A., *Phys. Rev. D*, **81** (2010) 103530.
- [12] LACKI B. C., and BEACOM J. F., *Astrophys. J.*, **720** (2010) L67.
- [13] SHANDERA S., ERICKCEK A. L., SCOTT P., and GALARZA J. Y., arXiv: 1211.7361
- [14] LI F., ERICKCEK A. L. and LAW N. M., arXiv: 1202.1284.
- [15] JUNGMAN G., KAMIONKOWSKI M. and GRIEST K., *Phys. Rep.*, **267** (1996) 195.
- [16] BERTONE G., HOOPER D. and SILK J., *Phys. Rep.*, **405** (2005) 279.
- [17] BERGSTROM L., *New J. Phys.*, **11** (2009) 105006.
- [18] TAKAYAMA F. and YAMAGUCHI M., *Phys. Lett. B*, **85** (2000) 388.
- [19] ARVANITAKI A. ET AL, *Phys. Rev. D*, **79** (2009) 105022.
- [20] NAVARRO F., FRENK C. S. and WHITE S. D. M., *Astrophys. J.*, **490** (1997) 493.
- [21] BAHCALL J. N. and SONEIRA R. M., *Astrophys. J. Suppl.*, **44** (1980) 73.
- [22] EINASTO J., *Trudy Astrophys. Inst. Alma-Ata*, **5** (1965) 87.
- [23] SALUCCI P. ET AL, *MNRAS*, **402** (2012) 2034.
- [24] BOER W. and WEBER M., *JCAP*, **1104** (2011) 002.
- [25] BERNAL N. and RUIZ S. P., *JCAP*, **1201** (2012) 006.
- [26] FILLMORE J. A. and GOLDBREICH P., *Astrophys. J.*, **281** (1984) 1.
- [27] BERTSCHINGER E., *Astrophys. J. Suppl.*, **58** (1985) 39.
- [28] KOMATSU E. ET AL, *Astrophys. J. Suppl.*, **192** (2011) 18.
- [29] CIRELLI M., MOULIN E., PANCI P., SERPICO P. D. and VIANA A., arXiv:1205.5283.
- [30] DUGGER L., JELTEMA T. E. and PROFUMO S., *JCAP*, **12** (2010) 015.
- [31] ZHANG L., WENIGER C., MACCIONE L., REDONDO J. and SIGL G., *JCAP*, **06** (2010) 027.
- [32] IBARRA A., TRAN D. and WENIGER C., *JCAP*, **1001** (2010) 009.
- [33] CIRELLI M., PANCI P. and SERPICO P. D., *Nucl. Phys. B*, **840** (2010) 284.
- [34] MASINA I., PANCI P. and SANNINO F., arXiv: 1205.5918.
- [35] BERTONE G., BUCHMULLER W., COVI L. and IBARRA A., *JCAP*, **0711** (2007) 003.
- [36] HUTSI G., HEKTOR A. and RAIDAL M., *JCAP*, **7** (2010) 8.
- [37] HUANG X., VERTONGEN G. and WENIGER C., arXiv: 1110.6236.
- [38] ACKERMANN M. ET AL, arXiv: 1205.6474.
- [39] CHEN X. and KAMIONKOWSKI M., *Phys. Rev. D*, **70** (2004) 043502.
- [40] ZHANG L., CHEN X., KAMIONKOWSKI M., SI Z. and ZHENG Z., *Phys. Rev. D*, **76** (2007) 061301.
- [41] DUNKELY L. ET AL, *Astrophys. J. Suppl.*, **180** (2009) 306
- [42] KUO C. L. ET AL, *Astrophys. J.*, **664** (2007) 687.
- [43] MONTROY T. E. ET AL, *Astrophys. J.*, **647** (2006) 813.
- [44] READHEAD A. C. S. ET AL, *Astrophys. J.*, **609** (2004) 498.
- [45] KUO C. L. ET AL, *MNRAS*, **353** (2004) L732.
- [46] ADRIANI O. ET AL, *Nature*, **458** (2009) 607.
- [47] IBARRA A. and TRAN D., *JCAP*, **0902** (2009) 021.
- [48] IBARRA A. and TRAN D., *Phys. Rev. D*, **79** (2009) 023512.
- [49] CHANG J. ET AL, *Nature*, **456** (2008) 362.
- [50] LIU J., YIN P. and ZHU S., *Phys. Rev. D*, **79** (2009) 063522.